reduced, but for $\theta\phi$, $\phi\theta$, and $\phi\phi$ polarizations TCD, although negative, tends to decrease further. So at lower frequencies the cross-polarization properties of the loop and the clutter sources tend to be comparable. At high frequencies the clutter cross-polarizations are stronger than those of the test target. This is in accordance with the belief that when the correlation lengths in the random medium are appreciable fractions of wavelength, the cross-polarization returns are strong. Depending upon the target and its orientation, the cross-polarization return may easily be lost in the clutter. To draw more conclusions, a more detailed parametric study and optimization are necessary. This will be represented later.

REFERENCES

1. J. Richard Huynen, *Phenomenological Theory of Radar Targets*, Drukkerij Bronder-offset, N. v., Rotterdam.
2. Alexander B. Kotsinski and Wolfgang M. Boerner, "On Foundations of Radar Polarimetry," *IEEE Trans. Antennas Propagat.*, Vol. AP-34, Dec. 1966, pp. 1395–1404 (comments by Harry Mieras and reply by the authors, *ibid.*, pp. 1470–1473).
3. Glendon C. McCormick and Archibald Hendry, "Optimal Polarisations for Partially Polarised Backscatter," *IEEE Trans. Antennas Propagat.*, Vol. AP-33, Jan. 1985, pp. 33–39.
4. George A. Ioannidis and David E. Hammers, "Optimum Antenna Polarizations for Target Discrimination in Clutter," *IEEE Trans. Antennas Propagat.*, Vol. AP-27, May 1979, pp. 357–363.
5. Alexander B. Kostinski and Wolfgang M. Boerner, "On the Polarimetric Contrast Optimization," *IEEE Trans. Antennas Propagat.*, Vol. AP-35, August 1987, pp. 988–991.
6. L. Tsang, J. A. Kong, and R. T. Shin, *Theory of Microwave Remote Sensing*, Wiley, New York, 1985.
7. J. W. Crispin and K. M. Siegel, *Methods of RCS Analysis*, Academic, New York, 1968, Chap. 3.
8. Michael A. Zuniga, Tarek M. Habashy, and Jin Au Kong, "*Active Remote Sensing of Layered Random Medium*," *IEEE Trans. Geosci. Electron.*, Vol. GE-19, Oct. 1979, pp. 296–302.
9. Michael A. Zuniga, "Theoretical Studies for Microwave Remote Sensing of Layered Random Media," Ph.D. thesis, Dept. of Physics, MIT, Jan. 1980.
10. M. Borgeaud, R. T. Shin, and J. A. Kong, "Theoretical Models for Polarimetric Radar Clutter," *J. Electromag. Waves Appl.* Vol. 1, No. 1, 1987, pp. 73–89.

Received 11-7-90

Microwave and Optical Technology Letters, 4/5, 179–181

CCC 0895-2477/91/050179-03$04.00

NUMERICAL ANALYSIS OF AN OPTICAL COUPLER COMPOSED OF THREE-CHANNEL WAVEGUIDES WITH DIFFERENT CORE SIZES

Hiroshi Kubo and Kiyotoshi Yasumoto
Department of Computer Science and Communication Engineering
Kyushu University 36, Hakozaki 6-10-1
Fukuoka 812, Japan

KEY TERMS

Optical coupler, three-channel waveguides, numerical analysis, mode-matching method

ABSTRACT

An optical coupler composed of three-channel waveguides with different core sizes is analyzed numerically. Dispersion relations and field distributions are presented for the lowest three modes in the coupler. It is shown that the geometric parameter of the coupler can be optimized so as to satisfy the condition for a maximum power transfer efficiency.

1. INTRODUCTION

Recently there has been interest in the study of three-parallel-waveguides couplers [1, 2]. The three-parallel-waveguides coupler eliminates the need for bends and has a sharp transfer characteristic that is superior to that of a two-parallel-waveguides couplers [3]. Characteristics of a coupler composed of identical three-channel waveguides have been analyzed by several methods [4, 5]. Results of these analyses show that the differences between the propagation constants of the lowest three modes are not generally equal, so that the high power transfer efficiency from one outer waveguide to the other cannot be obtained. In this article, the three-guides coupler composed of nonidentical center and outer-channel waveguides is investigated numerically, using the mode-matching method developed by Yasuura [6]. This method, in which the convergency of the solutions is ensured theoretically, has been successfully applied to guiding problems in several dielectric waveguides [5, 7]. For the purpose of analyzing the modal property accurately, we shall use the mode-matching method based on the hybrid-modal representation. It is shown that the differences between the propagation constants of the lowest three modes can be made equal by varying the depth of the center waveguide. The numerical results of the dispersion relations and field distributions are presented for the three modes in the coupler with the optimum waveguide parameter. The time factor is assumed to be of the form $\exp(-i\omega t)$.

2. FORMULATION OF THE PROBLEM

The geometry considered here is a three-channel waveguide, as shown in Figure 1(a), which is composed of the covered region S_1, the guided region S_2, and the substrate region S_3, and is uniform in the z direction. The refractive indices of the three regions are n_1, n_2, and n_3 ($n_1 \leq n_3 \leq n_2$), respectively.

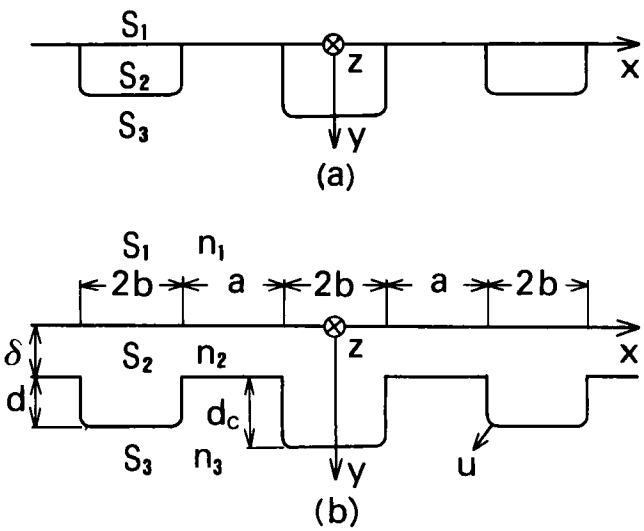

Figure 1 Geometry of (a) three-channel waveguides and (b) three-parallel thin-film waveguides

This configuration may be considered as a special case of a similar thin-film structure shown in Figure 1(b), and is obtained by reducing the thickness δ of the slab layer in the region S_2 to zero ($\delta \to 0$). Thus we shall develop our discussion on the configuration of Figure 1(b) in what follows. The boundary surface C_{23} between S_2 and S_3 is given by

$$y = \xi(x) = \begin{cases} \delta, & \text{for } b < |x| < a + b \text{ and } a + 3b < |x|, \\ d_c\{1 - (|x|/b)^{10}\}^{\frac{1}{4}}, & \text{for } 0 \le |x| \le b, \\ d\{1 - (|x - a - 2b|/b)^{10}\}^{\frac{1}{4}}, & \text{for } a + b \\ & \le |x| \le a + 3b, \end{cases} \quad (1)$$

where the heights of the center waveguide and the outer waveguides are denoted by d_c and d, respectively. The guided waves in this type of dielectric waveguide can be represented by a linear combination of TE_y wave with $E_y \equiv 0$ and the TM_y wave with $H_y \equiv 0$. They are referred to as the HE_y (or EH_y) mode when the TE_y (or TM_y) wave component is dominant. For the TE_y (or TM_y) wave component, E_x (or H_x) can be adopted as a leading field and is denoted by $\Psi_j(x, y)$ [or $\Phi_j(x, y)$] ($j = 1, 2, 3$). Then $\Psi_j(x, y)$ and $\Phi_j(x, y)$ satisfy the Helmholtz equations

$$\left(\frac{\partial^2}{\partial x^2} + \frac{\partial^2}{\partial y^2} + k^2 n_j^2 - \beta^2\right)\begin{bmatrix}\Psi_j(x, y) \\ \Phi_j(x, y)\end{bmatrix} = 0, \quad j = 1, 2, 3, \quad (2)$$

where k is the wavenumber in free space and β is a real propagation constant in the z direction. Referring to the mode-matching method for unbounded objects [6], $\Psi_j(x, y)$ and $\Phi_j(x, y)$ in the regions S_2 and S_3 can be approximated by the finite Fourier integral as follows:

$$\begin{bmatrix}\Psi_{jw}(x, y) \\ \Phi_{jw}(x, y)\end{bmatrix} = \frac{1}{2\pi}\int_{-w}^{w}\begin{bmatrix}\psi_{jw}(h) \\ \phi_{jw}(h)\end{bmatrix} p_j(h, y)\exp(ihx)\,dh, \quad j = 2, 3, \quad (3)$$

with

$$p_2(h, y) = \frac{1}{\gamma}[\exp\{-i\kappa_2(h)y\} + R(h)\exp\{i\kappa_2(h)y\}], \quad (4)$$

$$p_3(h, y) = \frac{1}{\gamma}[\exp\{i\kappa_3(h)y\}], \quad (5)$$

$$R(h) = \begin{cases} \dfrac{\kappa_2(h) - \kappa_1(h)}{\kappa_2(h) + \kappa_1(h)}, & \text{for } \Psi_{jw}(x, y), \\ \dfrac{n_1^2\kappa_2(h) - n_2^2\kappa_1(h)}{n_1^2\kappa_2(h) + n_2^2\kappa_1(h)}, & \text{for } \Phi_{jw}(x, y), \end{cases} \quad (6)$$

$$\gamma = \begin{cases} 1, & \text{for } \Psi_{jw}(x, y), \\ \omega\mu d & \text{for } \Phi_{jw}(x, y), \end{cases} \quad (7)$$

$$\kappa_j(h) = (k^2 n_j^2 - \beta^2 - h^2)^{\frac{1}{4}}, \quad j = 2, 3, \quad (8)$$

where μ is a permeability that is common in three regions, w is the bandwidth of the wavenumber in the x direction, $\psi_{jw}(x, y)$ and $\phi_{jw}(x, y)$ are the band-limited spatial spectra functions, and $\kappa_j(h)$ are positive real or positive imaginary. Note that the approximate wave functions $\Psi_{jw}(x, y)$ and $\Phi_{jw}(x, y)$ and their unknown spatial spectra $\psi_{jw}(h)$ and $\phi_{jw}(h)$ depend on the bandwidth w. Using the Maxwell equations, the remaining field components for the approximate TE_y and TM_y waves can be obtained in terms of the spectra $\psi_{jw}(h)$ and $\phi_{jw}(h)$. Taking a linear combination of the approximate TE_y and TM_y wave components, the approximate electric and magnetic field vectors $\mathbf{E}_{jw}$ and $\mathbf{H}_{jw}$ of the hybrid guided waves are deduced.

Using the mode-matching method, we can find the approximate wave functions $\{\Psi_{jw}(x, y)\}$ and $\{\Phi_{jw}(x, y)\}$ ($j = 2, 3$), which converge uniformly to the true fields $\Psi_j(x, y)$ and $\Phi_j(x, y)$ as the bandwidth w is increased. Now we shall describe how to obtain the unknown spectra $\Psi_{jw}(h)$ and $\phi_{jw}(h)$ and the propagation constant β. The approximate field vectors $\mathbf{E}_{jw}$ and $\mathbf{H}_{jw}$ are matched to the boundary conditions on the surface C_{23} in the sense of least squares. For this purpose, we introduce the mean square boundary residual Ω_w on C_{23} as follows:

$$\Omega_w = \int_{-\infty}^{\infty}(|\mathbf{u}(x) \times [\mathbf{E}_{2w}\{x, \xi(x)\} - \mathbf{E}_{3w}\{x, \xi(x)\}]|^2 + \alpha^2|\mathbf{u}(x) \times [\mathbf{H}_{2w}\{x, \xi(x)\} - \mathbf{H}_{3w}\{x, \xi(x)\}]|^2)\,dx, \quad (9)$$

where $\alpha = \omega\mu/n_2 k$ is the intrinsic impedance of medium n_2 and $\mathbf{u}(x)$ is the unit normal vector on C_{23}. The value of Ω_w should be minimized with respect to $\{\psi_{jw}(h), \phi_{jw}(h); j = 2, 3\}$ under suitable constraints. The spectral form of the constraints is given by

$$\frac{1}{2\pi}\int_{-w}^{w}\mathbf{X}^*(h)\cdot\mathbf{F}(h)\,dh = 1, \quad (10)$$

where $\mathbf{X}(h)$ is a row vector defined as

$$\mathbf{X}(h) = [\psi_{2w}(h) - \psi_{3w}(h)\phi_{2w}(h) - \phi_{3w}(h)]. \quad (11)$$

The explicit expression for column vector $\mathbf{F}(h)$ was given elsewhere [5]. Introducing a Lagrange undetermined multiplier λ_w, we consider the quantity

$$\Gamma_w = \Omega_w + \lambda_w^*\left[\frac{1}{2\pi}\int_{-w}^{w}\mathbf{X}(h)\cdot\mathbf{F}(h)\,dh - 1\right] + \lambda_w\left[\frac{1}{2\pi}\int_{-w}^{w}\mathbf{X}^*(h)\cdot\mathbf{F}^*(h)\,dh - 1\right], \quad (12)$$

where the asterick means the complex conjugate of the indicated functions. Letting the first derivatives of Γ_w with respect to $\psi_{jw}^*(h)$, $\phi_{jw}^*(h)$ ($j = 2, 3$), and λ_w^* be zero, we obtain a set of equations for $\mathbf{X}(h)$ to be solved numerically.

$\mathbf{X}(h)$ and λ_w are obtained by solving the set of equations for property fixed values of β, k, and w. Letting $\Omega_{w,\min}$ be the minimum value of Ω_w for such solutions, we have the relation

$$\lambda_w(\beta, k) = -\Omega_{w,\min}(\beta, k). \quad (13)$$

Then if we calculate λ_w by varying β for fixed k and w, the approximate propagation constant $\beta_w(k)$ can be obtained by the value of β which minimizes $-\lambda_w$. Using the value of $\beta_w(k)$ and the corresponding solutions for $\mathbf{X}(h)$, the approximate electric and magnetic fields of the guided waves can be numerically calculated.

3. NUMERICAL RESULTS

We show numerical results on the modal property in the three-channel waveguides of Figure 1(a), with the geometric parameters $\delta = 0$, $a/d = 3.4 \sim 3.8$, $b/d = 1.0$, and $d_c/d = 1.000 \sim 1.003$, and with the indices $n_1 = 1.00$, $n_2 = 2.23$, and $n_3 = 2.20$. After confirming the convergency of the numerical solutions, the bandwidth w for the finite Fourier integral and the number of the division N for the numerical integration are chosen as $wd = 10.0$ and $N = 40$.

To obtain a maximum power transfer efficiency from one outer waveguide to the other, $\Delta\beta_{01}d$ must be equal to $\Delta\beta_{12}d$ [8]. $\Delta\beta_{01}d$ denotes the difference between propagation constants of HE_{y0} and HE_{y1} modes, and $\Delta\beta_{12}d$ denotes the difference between propagation constants of HE_{y1} and HE_{y2} modes. HE_{y0}, HE_{y1}, and HE_{y2} are the lowest even mode, the lowest odd mode, and the second-lowest even mode in HE_y, respectively. Figure 2 shows the differences between the propagation constants as a function of the depth d_c of the center waveguide for $a/d = 3.4$, 3.6, and 3.8, with $kd = 5.8$. It is seen that ratio of $\Delta\beta_{01}d$ to $\Delta\beta_{12}d$ can be adjustable by varying d_c. When the depth of the center waveguide is chosen as $d_c/d = 1.0020$, 1.0018, and 1.0014 for $a/d = 3.4$, 3.6, and 3.8, respectively, $\Delta\beta_{01}d$ is equal to $\Delta\beta_{12}d$. Suppose that one outer waveguide of the coupler with the above geometric parameter is excited. Then the HE_{y0} and HE_{y2} modes come to be in phase each other and in antiphase with the HE_{y1} mode, and the power in one outer waveguide transfers to the other at a distance $L = \pi/\Delta\beta_{01} = \pi/\Delta\beta_{12}$.

Figure 3 shows the dispersion curves for the HE_{y0}, HE_{y1}, HE_{y2}, and EH_{y0} modes with $a/d = 3.8$, $d_c/d = 1.0014$. The EH_{y0} mode is the lowest even mode in EH_y. The three channel waveguides can be used as a directional coupler in the frequency range marked by Δkd, where only the HE_{y0}, HE_{y1}, and HE_{y2} modes with the same polarization can propagate without loss.

The field distributions of $E_x(x, y)$ for the HE_{y0}, HE_{y1}, and HE_{y2} modes are plotted in Figure 4 as a function of x/d for $y/d = 0.5$, with $a/d = 3.8$, $d_c/d = 1.0014$, and $kd = 5.8$. The amplitude of field is normalized by the maximum value.

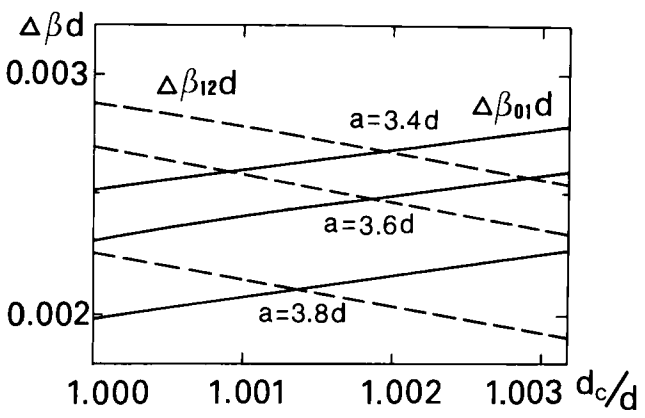

Figure 2 Differences between propagation constants as a function of the depth of the center waveguide d_c for $a/d = 3.4$, 3.6, and 3.8, with $kd = 5.8$, $b/d = 1.0$, $n_1 = 1.00$, $n_2 = 2.23$, and $n_3 = 2.20$

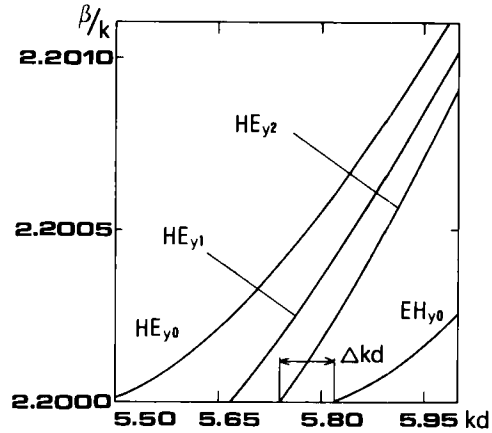

Figure 3 Dispersion curves of the HE_{y0}, HE_{y1}, HE_{y2}, and EH_{y0} modes in the three-channel waveguides with $a/d = 3.8$, $d_c/d = 1.0014$, $b/d = 1$, $n_1 = 1.00$, $n_2 = 2.23$, and $n_3 = 2.20$

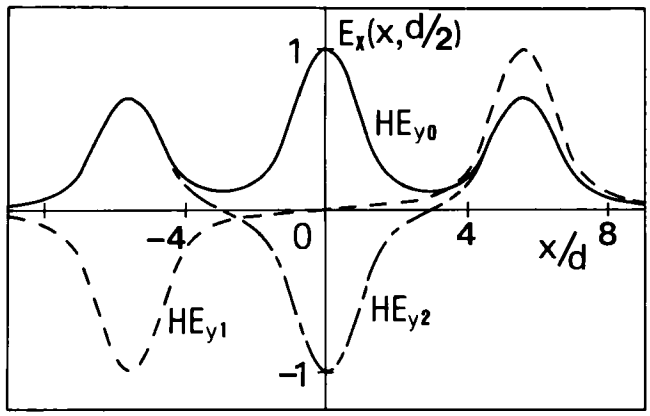

Figure 4 Field distributions of $E_x(x, y)$ for the HE_{y0} (solid line), HE_{y1} (dashed line), and HE_{y2} (long-dash–short dash line) modes in the three-channel waveguides, as a function x/d for $y/d = 0.5$ and $kd = 5.8$, with $a/d = 3.8$, $d_c/d = 1.0014$, $b/d = 1.0$, $n_1 = 1.00$, $n_2 = 2.23$, and $n_3 = 2.20$

4. CONCLUSION

The guided waves in the three-guides coupler composed of nonidentical center and outer channel waveguides have been analyzed numerically by using the mode-matching method. The phase relation was shown to have maximum power transfer efficiency when the depth of the center waveguide was property set. The precise numerical results of dispersion relations are near the cutoff were obtained and the available frequency range was discussed.

REFERENCES

1. J. P. Donnelly, N. L. Demeo, Jr., and G. A. Ferrante, "Three-Guide Optical Couplers in GaAs," *IEEE J. Lightwave Technol.*, Vol. LT-1, June 1983, pp. 417–424.
2. Y. Cai, T. Mizumoto, and Y. Naito, "Analysis of the Coupling Characteristics of a Tapered Three-Guide Coupled System," *IEEE J. Lightwave Technol.*, Vol. LT-8, Oct. 1990, pp. 1621–1629.
3. H. A. Haus and C. G. Fonstad, Jr., "Three-Waveguide Couplers for Improved Sampling and Filtering," *IEEE J. Quantum Electron.*, Vol. QE-17, Dec. 1981, pp. 2321–2325.
4. A. N. Kaul, K. Thyagarajan, and A. Kumar, "Coupling Characteristics of a Three Channel Waveguide Directional Coupler," *Opt. Commun.*, Vol. 56, Nov. 1985, pp. 95–99.
5. H. Kubo and K. Yasumoto, "Numerical Analysis of Three-Parallel Embedded Waveguides," *IEEE J. Lightwave Technol.*, Vol. LT-7, Dec. 1989, pp. 1924–1931.
6. K. Yasuura, K. Shimohara, and T. Miyamoto, "Numerical Analysis of a Thin-Film Waveguide by Mode-Matching Method," *J. Opt. Soc. Am.*, Vol. 70, Dec. 1980, pp. 183–191.

7. K. Yasumoto, H. Kubo, and Y. Itoh, "Numerical Analysis of a Multilayered Dielectric Waveguide with a Periodic Surface," *Microwave Opt. Technol. Lett.*, Vol. 2, Sept. 1981, pp. 317–319.
8. J. P. Donnelly, H. A. Haus, and N. Whitaker "Symmetric Three-Guide Optical Coupler with Nonidentical Center and Outside Guides," *IEEE J. Quantum Electron.*, Vol. QE-23, April 1987, pp. 401–406.

Received 12-12-90

Microwave and Optical Technology Letters, 4/5, 181–184

CCC 0895-2477/91/050181-04$04.00

COMPUTATIONS OF THE DIFFRACTION EFFECT AND THE NONLINEAR EFFECT ON SPATIAL SOLITONS IN NONLINEAR PLANAR WAVEGUIDES*

Jie-Ren Bian and Andrew K. Chan
Department of Electrical Engineering
Texas A&M University
College Station, Texas 77843

KEY TERMS

Spatial soliton, nonlinear Schrödinger equation, coupled soliton, lossy waveguide

ABSTRACT

The nonlinear effect and the diffraction effect on a spatial soliton are isolated by rewriting the nonlinear Schrödinger equation into a form of the linear Schrödinger equation with a nonlinear potential. Numerical results on these effects are obtained for a fundamental spatial soliton, a second-order spatial soliton, and two coupled solitons in a parallel-plate waveguide. The effects of waveguide loss are also included.

1. INTRODUCTION

Research in optical soliton propagation has gained much attention in recent years because of its potential application to high-bit-rate transmission systems. The shape maintenance property and the particle-like property possessed by a soliton make it an ideal vehicle for two-way long-distance high-repetition-rate pulse communication. For this reason, virtually all research work on the optical soliton for communication uses the optical soliton to represent the envelope of a time-domain signal. Recently, the spatial soliton has been observed in CS_2 liquid [1–3] and in a single-mode glass waveguide [4]. In fact, experimental observations on two spatial solitons interacting with each other have also been reported in [4].

Although the shape-maintenance property of a fundamental soliton is well known, it is only qualitatively explained in the literature that the dispersive effect is balanced perfectly by the self-focusing effect due to the nonlinearity of the medium. No quantitative analysis, theoretical or numerical, on the evolution of a spatial soliton propagating in a nonlinear planar waveguide has been found in the literature. In this article we will rewrite the nonlinear Schrödinger equation, which governs the propagation of a spatial soliton in a parallel-plate waveguide, into the form of a linear Schrödinger equation with a nonlinear potential function proportional to the square of the field amplitude. The traditional momentum and energy operators in quantum mechanics will be applied to the equation and we will derive an effective nonlinear force and an effective diffraction force acting simultaneously on the soliton. In this way, the shape changes of a spatial soliton can be directly related to the imbalance between these forces. We will use this scheme to study the shape changes of a fundamental spatial soliton, a second-order spatial soliton, and the interactions of two spatial solitons in lossless and lossy waveguides. In addition, we will make observations on the evolution of a Gaussian beam in a nonlinear parallel-plate waveguide.

*This project is supported by Texas Higher Education Coordinating Board under Grants No. 32123-70030 and No. 32130-70440.

2. THEORY

In the presence of a third-order nonlinearity in a medium, the electromagnetic wave equation is modified to become [5, 6]

$$\nabla^2\mathbf{E} - \frac{\varepsilon_0}{c^2}\frac{\partial^2\mathbf{E}}{\partial t^2} - \frac{\varepsilon_2}{c^2}\frac{\partial^2}{\partial t^2}(|\mathbf{E}|^2\mathbf{E}) = 0, \tag{1}$$

where $\varepsilon = \varepsilon_0 + \varepsilon_2|\mathbf{E}|^2$ is the nonlinear dielectric constant. For weak nonlinearity, $(\varepsilon_2/\varepsilon_0)|\mathbf{E}|^2 \ll 1$. The optical wave is assumed to be linearly polarized of frequency ω, and it propagates along the z axis. The electric field is expressed as

$$\mathbf{E} = \hat{\mathbf{e}}_x \tfrac{1}{2}(E' e^{i(kz-\omega t)} + \text{c.c.}), \tag{2}$$

where c.c. stands for complex conjugate of the term preceding the symbol, $k = \varepsilon_0^{1/2}(\omega/c)$ is the wave number in a linear medium characterized by ε_0 and E' is the slow varying complex envelope of the field. By substitution of (2) into (1) and neglecting the third-harmonic terms and the second z- derivative of E' (i.e., we assume the characteristic distance of the change of E' in the z direction is much larger than the wavelength), we have

$$2ik\frac{\partial E'}{\partial z} + (\nabla_x^2 + \nabla_y^2)E' + \frac{\varepsilon_2 k^2}{\varepsilon_0}|E'|^2E' = 0. \tag{3}$$

In a two-dimensional medium with a nonlinear refractive index n_2, Eq. (3) becomes

$$2ik\frac{\partial E'}{\partial z} + \frac{\partial^2 E'}{\partial x^2} + k^2\frac{n_2^2}{n_0^2}|E'|^2E' = 0. \tag{4}$$

Here n_0 represents the linear part of refractive index and n_2 the nonlinear part.

Within certain power constrains, the solution of (4) is a spatial soliton which can exist in a slab waveguide with its width being much larger than the transverse mode size of the soliton. Under this condition, the self-focusing effect occurs only in the x direction. Let a_0 represents the width of soliton and w the dimension of its transverse mode size. Using $x' = xa_0$, $z = \xi L_D$, $E' = u\sqrt{P_0}$, Eq. (4) becomes

$$i\frac{\partial u}{\partial \xi} + \frac{1}{2}\frac{\partial^2 u}{\partial x'^2} + N^2|u|^2u = 0, \tag{5}$$

where P_0 is the initial peak power, $L_D = ka_0^2$ is the diffraction length, ξ is the normalized distance, $Z_0 = (\pi/2)L_D$ is the soliton period in the waveguide, and $N^2 = P_0k^2n_2^2/n_0^2$ is the